Hindawi
International Journal of Electrochemistry
Volume 2019, Article ID 8796958, 8 pages
https://doi.org/10.1155/2019/8796958

Research Article

Arc Thermal Spray NiCr20 Alloy Coating: Fabrication, Sealant, Heat Treatment, Wear, and Corrosion Resistances

Van Tuan Nguyen,[1] Quy Le Thu,[2] Tuan Anh Nguyen ,[1] Quoc Cuong Ly,[1] Ly Pham Thi,[1] Ha Pham Thi,[1] and Thanh Dinh Thi Mai[1]

[1]*Institute for Tropical Technology, Vietnam Academy of Science and Technology, 18, Hoang Quoc Viet, Cau Giay, Hanoi, Vietnam*
[2]*National Key Laboratory for Welding and Surface treatment Technologies, National Research Institute of Mechanical Engineering, No.4 Pham Van Dong, Cau Giay, Hanoi, Vietnam*

Correspondence should be addressed to Tuan Anh Nguyen; ntanh@itt.vast.vn

Received 5 November 2018; Accepted 1 January 2019; Published 27 January 2019

Academic Editor: Gerd-Uwe Flechsig

This study presents the effect of heat treatment on porosity, phase composition, microhardness, and wear and corrosion resistances of the thermal sprayed NiCr20 coating after sealing with aluminum phosphate. The annealing temperatures were varied in a range of 400 to 1000°C. The obtained results indicated the porosity of coating decreased with increasing the annealing temperature. After treatment at temperatures in range of 800-1000°C, more than 90% of initial pores in the coating were successfully filled with the sealants. The XRD data revealed not only the formation of new phases of other compounds, but also the interaction between coating and sealant. After heat treatment, wear resistance of coating was 12 times higher than that without heat treatment. The corrosion test in H_2SO_4 solution indicated that the presence of sealant in coatings increased their corrosion resistance. From these findings, application of these NiCr20 coatings to protect steel against wear and corrosion appears very promising.

1. Introduction

For the thermal spray coatings in corrosive environments, their intrinsic porosity could facilitate the ingress of corrosive agents, resulting in the initiation of corrosion leading to the coating delamination. The porous structure not only deteriorates their corrosion resistance, but also decreases their mechanical properties and consequently reduces their wear resistance [1]. Thus, the post-heat treatment after spraying process is necessary. This posttreatment process could be carried out by using various techniques, such as the laser or electron-beam surface melting, alloying method, hot isostatic pressing (HIP), chemical vapor deposition (CVD), and chemical vapor infiltration (CVI). However, these techniques are costly and require complex equipment. Other effective posttreatments, like the impregnation technique using polymers, inorganic compounds, or molten metals, have been applied [1].

It was reported in literature that aluminum phosphate sealant could infiltrate deeply into plasma-sprayed coating layers, inhibit the formation of pores, and increase the abrasion resistance of the coatings [1–7]. The influence of temperature on porosity and wear resistance of thermal coating after sealing with aluminum phosphate has been also reported [8–10].

Aluminum phosphate sealed NiCr alloy coatings have been widely applied for corrosion protection at high temperatures [11–14]. However, the effect of heat treated temperature on the adhesive strength, phase composition, and microstructures of coatings has been reported mostly for the NiCr20 alloy coatings. There was a lack of information about the effect of heat treatment on property and structure of the aluminum phosphate sealed NiCr20 coatings.

In this study, we present our research on the effect of heat treatment on porosity, phase composition, microhardness, and wear and corrosion resistances of the thermal sprayed NiCr20 coating after sealing with aluminum phosphate.

Table 1: Technological parameters for sprayed NiCr alloy coating.

Spray modes	Technological parameters
Spray angle (°)	90
Spray distance (mm)	100
Pneumatic pressure (atm)	4.2 ÷ 4.5
Arc voltage (V)	33
DC current (A)	200
Nozzles moving speed (mm/s)	30
Coating thickness (mm)	≈1

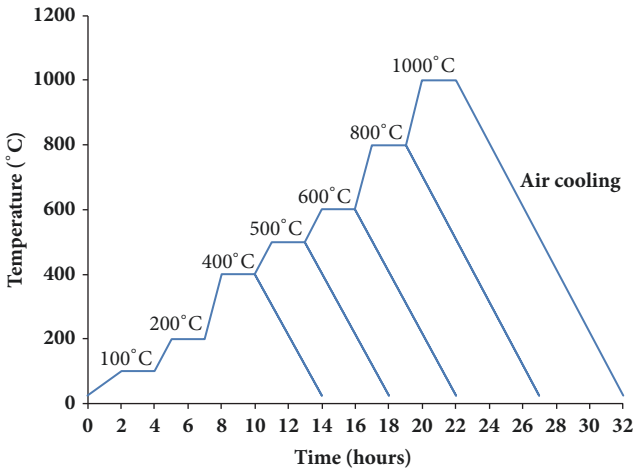

Figure 1: Temperature diagram of heat treatment procedure for sealing samples.

2. Experimental

2.1. Sample Preparation. Aluminum phosphate was prepared using orthophosphoric acid (H_3PO_4, 85%) and aluminum hydroxide powder ($Al(OH)_3$), with 2.3 molar ratio of P/Al. The reaction took place at 120°C till clear solution is obtained. The obtained aluminum phosphate solution has the viscosity (η) of 177.36 s and the density (ρ) of 1.58 g.cm^{-3}.

NiCr20 alloy coatings have been fabricated by spraying with electric-arc equipment OSU-HESSLER 300A (OSU Hessler GmbH & Co., Germany). The optimized spraying parameters are shown in Table 1.

The NiCr20 alloy wires have their diameter of 2 mm and their chemical composition of 79.39% Ni, 18.16% Cr, 0.9% Si, 0.26% Ti, 0.73% Mn, and 0.56% Fe. The metallic is C45 carbon-steels (round shape Ø 50 mm, thickness 3 mm). The coating thickness is about 1000 μm.

To seal the NiCr20 coating samples, the aluminum phosphate prepared solution is used and stabilized during 12 hours at room temperature and then heat treated with the below continuous steps (Figure 1).

2.2. Coating Characterization. After heat treatment, the surface of coating samples, except the one exposed to electrolyte (for corrosion evaluation), was sealed with an epoxy resin in PVC plastic molds. After epoxy curing, the unsealed surface was wet-polished using SiC papers (grade down from #100 to #2000 sizes). After polishing, the samples were rinsed and sonicated in ultrasonic cleaning equipment. The samples were then dried in vacuum at 50°C.

Table 2: Denotation of the studied samples in heat treatment.

Samples	Annealing temperature, °C				
	400	500	600	800	1000
Aluminum phosphate	PA4	PA5	PA6	PA8	PA10
Unsealed NiCr20	NC4	NC5	NC6	NC8	NC10
Sealed NiCr20	NA4	NA5	NA6	NA8	NA10

For comparative studies on the effect of annealing temperature, Table 2 presents the denotation of the studied samples in heat treatment, for 3 different types of samples (such as aluminum sealant and unsealed and sealed NiCr20 alloy coatings).

The cross-sectional microstructure and porosity of coating samples have been analyzed using optical microscope Axiovert 40 Mat with imaging multiphase software.

To identify the possible phases that present in the coating, X-ray diffraction (SIEMENS D5005X-RAY instrument, Germany) has been used at temperature of 25°C, with 2θ angle scanning from 10° to 70° (scan step at 0.02°/s).

The wear resistance of the coatings was measured using TE-91 Precision Rotary Vacuum Tribometer (Phoenix Tribology Ltd, England), in accordance with the standard ASTM G99:2000 using 9CrSi dowel-steel with a hardness > 60HRC. The testing condition includes the load of 30N force, wear track radius of 20 mm, rotation speed of 382 rpm, sliding speed of 0.4 m/s, and testing duration of 900 s.

The hardness of coating (Vickers) was determined according to ISO 6507-2 standard, by using the microhardness tester FM-100 (Japan), with load of 300 g for 15 seconds [15].

The corrosion behaviour of the coatings in H_2SO_4 solution (pH 2) was determined using the AUTOLAB PGSTAT 302N. Two methods were used: electrochemical impedance spectroscopy (EIS) and linear polarization resistance (LPR) with a three-electrode system. The spraying samples were working electrodes, while the counter electrode and the reference electrode were a platinum electrode and a saturated calomel electrode (SCE), respectively. In the linear polarization resistance (LPR), the spraying coating samples were polarized around their (E_{ocp}) open circuit potential (−30 mV to 30 mV/SCE versus OCP) by a direct current (DC) signal at a scan rate of 2 mV/s, according to ASTM G3-14 standard. For EIS measurement, the spraying samples were polarized at ±5 mV around its open circuit potential (E_{ocp}) by an alternating current (AC) signal with its frequency ranging from 10^{-2} Hz to 10^5 Hz (7 points per decade) [16, 17].

3. Results and Discussion

3.1. XRD Analysis. Figures 2 and 3 present the XDR patterns of aluminum phosphates and sealed NiCr20 coatings, after heat treatment at different temperatures, respectively. Table 3 presents the denotation of the possible phases that present in

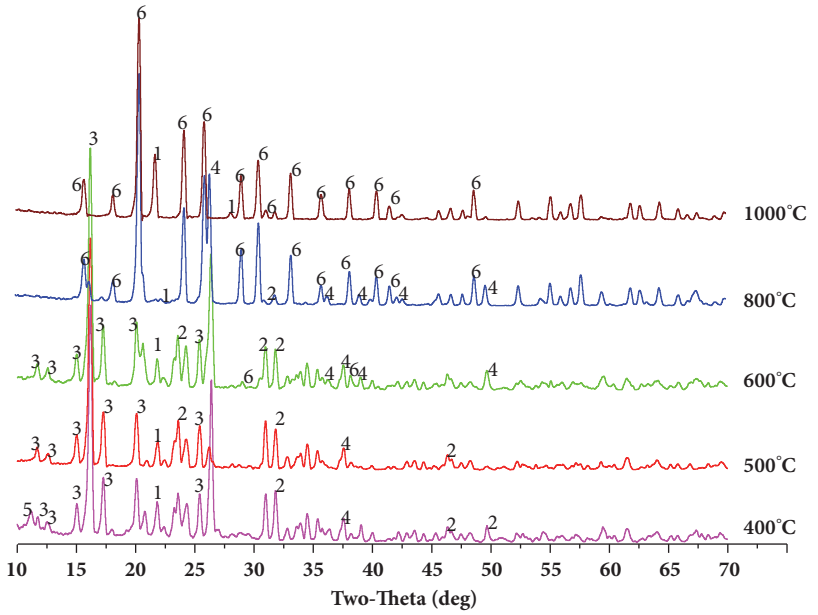

1- $AlPO_4$ (orthorhombic)
2- $Al_2P_6O_{18}$ (monoclinic)
3- $Al(PO_3)_3$ (N)
4- syn $AlPO_4$ (hexagonal)
5- $H_2AlO_3P_{10}.2H_2O$
6- $Al(PO_3)_3$ (cubic)

Figure 2: XRD patterns of aluminum phosphate samples with 2.3 molar ratio of P/Al, after treatment at different temperatures.

Table 3: Denotation of the possible phases present in samples.

Phase number	Phase composition
1	$AlPO_4$ (Orthorhombic)
2	$Al_2O_6P_{18}$ (Monoclinic)
3	$Al(PO_3)_3$(N)
4	Syn $AlPO_4$ (Hexagonal)
5	$H_2AlO_3P_{10}.2H_2O$
6	$Al(PO_3)_3$(Cubic)
7	Ni
8	$Al_{36}P_{36}O_{144}$ (Orthorhombic)
9	$Ni_3(PO_4)_2$ (Monoclinic)

samples. The possible phases that present in aluminum phosphate and sealed NiCr20 samples (at different temperatures) were shown in Tables 4 and 5, respectively.

3.1.1. Aluminum Phosphate Samples. For the aluminum phosphate samples (with 2.3 molar ratio of P/Al, Figure 2), the data indicated the presence of crystalline phase $AlPO_4$ (orthorhombic) in all testing samples at all range of temperature. However, their peak intensity of $AlPO_4$ (orthorhombic) has the highest value when annealing at 1000°C. In addition, the crystalline phase $AlPO_4$ (hexagonal) or syn $AlPO_4$ could not be detected at 1000°C for aluminum phosphate samples.

Above 400°C, as seen in Figure 2, the $H_2AlP_3O_{10}.2H_2O$ crystal no longer existed in the aluminum phosphate mixture. This result could be explained by the fact that $H_2AlP_3O_{10}.2H_2O$ crystalline phase has been transformed to the $Al_2O_6P_{18}$ and $Al(PO_3)_3$ crystalline phases through the following chemical reactions [18]:

$$H_2AlP_3O_{10}.2H_2O \xrightarrow{t^\circ \geq 400^\circ C(500^\circ C)} Al_2P_6O_{18} + 6H_2O \quad (1)$$

$$H_2AlP_3O_{10}.2H_2O \xrightarrow{t^\circ \geq 400^\circ C(500^\circ C)} Al(PO_3)_3 + 3H_2O \quad (2)$$

On the other hand, the $Al_2P_6O_{18}$ (monoclinic) crystal has been observed in aluminum phosphate mixture at 400, 500, and 600°C, but then it dispersed at higher temperatures. After treatment at 800°C, the $Al_2P_6O_{18}$ crystalline phase could be transformed into the $Al(PO_3)_3$ crystalline phase by the following chemical reaction [18]:

$$Al_2P_6O_{18} \xrightarrow{800^\circ C} Al(PO_3)_3 \quad (3)$$

Besides, the $Al(PO_3)_3$(N) crystalline phase was also found at temperatures in range from 400 to 800°C. This phase could be transformed into $Al(PO_3)_3$ (Cubic) crystal at 1000°C. The formation of $Al(PO_3)_3$ and $Al_2P_6O_{18}$ metaphosphate phases might enhance the wear resistance of the these thermal coatings [3–5].

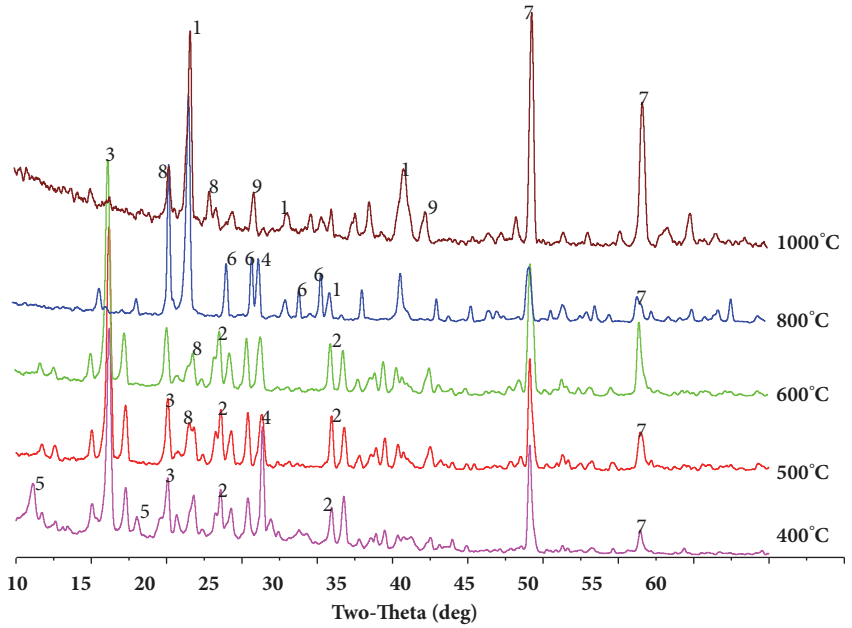

1- $AlPO_4$ (orthorhombic)
2- $Al_2P_6O_{18}$ (monoclinic)
3- $Al(PO_3)_3$(N)
4- syn $AlPO_4$(hexagonal)
5- $H_2AlO_3P_{10}.2H_2O$
6- $Al(PO_3)_3$(cubic)
7-Ni
8- $Al_{36}P_{36}O_{144}$(orthorhombic)
9- $Ni_3(PO_4)_2$(monoclinic)

Figure 3: XRD patterns of NiCr20 coating sealed with aluminum phosphate after treatment at different temperatures.

Table 4: Phase composition of aluminum phosphate with 2.3 molar ratio of P/Al, under different annealing temperatures.

Annealing temperature (°C)	Phase composition of aluminum phosphate					
	1	2	3	4	5	6
400	x	x	x	x	x	
500	x	x	x	x		
600	x	x	x	x		x
800	x		x	x		x
1000	x					x

Table 5: Phase composition of NA group of coating samples at different temperature.

Annealing temperature, °C	Phase composition of samples in NA group								
	1	2	3	4	5	6	7	8	9
400		x	x		x		x		
500		x	x	x			x	x	
600		x	x	x			x	x	
800	x		x	x		x	x		
1000	x	x					x		x

Table 6: Porosity values of sealed and unsealed coatings.

Samples	Initial porosity (%)	Sealed porosity (%)	Remaining porosity (%)	Sealed ratio (%)
NC4	11,45	7,56	3,89	65,73
NC5	13,13	9,23	3,9	70,42
NC6	14,95	11,31	3,6	75,07
NC8	13,19	9,97	3,21	75,48
NC10	13,83	11,33	2,5	82,11
NA4	13,02	11,09	1,93	84,99
NA5	16,31	13,91	2,4	84,89
NA6	11,93	9,81	2,12	81,63
NA8	15,25	13,84	1,41	90,71
NA10	14,89	13,46	1,43	90,32

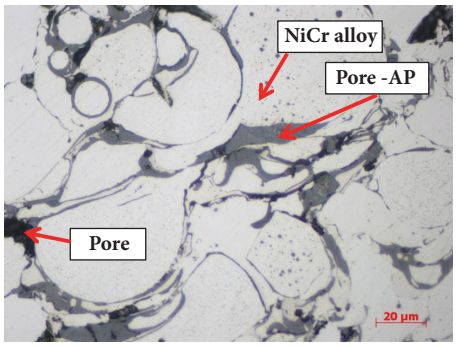

Figure 4: Cross-section image of NiCr alloy coating sealed by aluminum phosphate and heat-treated at 400°C.

Table 7: Microhardness values of prepared coating samples.

Samples	Microhardness HV 0.3, 15s
NA4	315 ± 31
NA5	284 ± 22
NA6	258 ± 32
NA8	255 ± 33
NA10	280 ± 22
NC4	275 ± 29
NC5	266 ± 23
NC6	274 ± 31
NC8	292 ± 43
NC10	275 ± 23

3.1.2. Sealed NiCr20 Spraying Samples. As shown in Table 5, for the sealed NiCr20 coatings, besides the similar crystalline phases of aluminum phosphate samples, other crystalline phases have been observed (Table 5), such that $Al_{36}P_{36}O_{144}$ phase was seen at the temperatures of 500, 600, and 1000°C. However, this phase was undetectable at 800°C, due to the formation of its amorphous state or the domination of other competing phases

In contrast to aluminum phosphate samples, the $AlPO_4$ (orthorhombic) crystalline phase could not be detected in the sealed NiCr20 coating samples at temperatures of 400, 500, and 600°C. In addition, at 1000°C, the $Ni_3(PO_4)_2$ crystalline phase was found on the coating, due to the following chemical interaction between the NiCr coating and aluminum phosphate [18].

$$291AlPO_4 + 3NiCr \xrightarrow{1000^\circ C} Ni_3(PO_4)_2 + Al_2Cr_3 + AlP_4\text{-}8\text{-}Al_{36}P_{36}O_{144} \quad (4)$$

3.2. Porosity and Microhardness Measurements. Figure 4 presents the cross-section of sealed NiCr alloy coating after heat-treatment at 400°C. As can be seen in this figure, almost all of open pores have been sealed. Porosity values for all prepared coatings are shown in Table 6.

As shown in Table 6, porosity values of unsealed coatings are in range from 3% to 4%, indicating the presence of remained pores at different treated temperatures. Their porosity decreased with increasing the annealing temperature, due to the increasing oxidation of metallic grains in the coatings, whereas, in case of sealed coatings, their porosity values are only in range from 1.4 to 2%, with the lowest value of 1.4% when treated at 800 to 1000°C. This result could be explained by the transformation of $H_2AlP_3O_{10}.2H_2O$ phase (NA4, at 400°C) into $Al_2P_6O_{18}$ phase (NA5, at 500°C) following the chemical reaction (1), thus leading to increase in the porosity by producing H_2O. The higher porosity values in NA6, NA8, and NA10 samples might be explained by interaction between sealant and neat coating through the diffusion phenomenon during heat treatment.

The microhardness is one of main factors influencing the wear resistance of coating. Table 7 presents the hardness values of prepared coating samples. As can be seen in this table, NA4 coating sample has the highest value; thus NA4 sample is expected to have the highest abrasion resistance. The highest value of microhardness could be attributed to the presence of $H_2AlO_3P_{10}$ crystalline phase in the coating (NA4 sample).

3.3. Wear Resistance Study. The weight loss could be used widely to evaluate the wear resistance of coating. Figure 5 shows the wear resistance of prepared coating samples. As shown in this figure, wear resistance of coating decreased with increasing the annealing temperatures. This result can

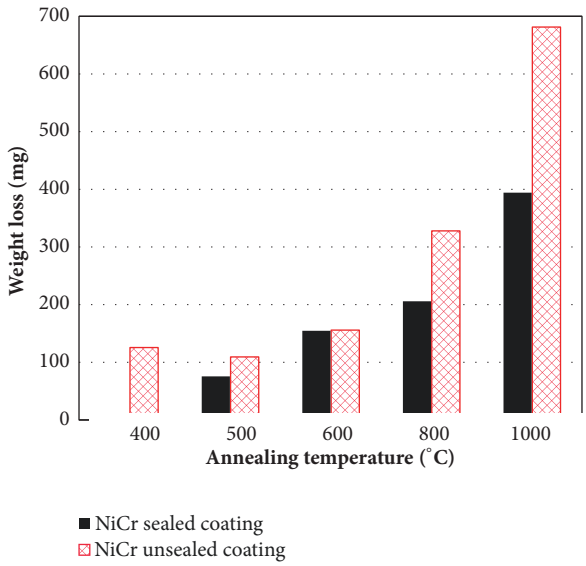

Figure 5: Wear resistance of coating samples at different temperatures.

be explained by the increasing oxidation when the annealing temperature increased, thus leading to reduction of the linkage between particles inside the coating. In addition, as mentioned in Section 3.1, H_2O molecules in $H_2AlP_3O_{10}.2H_2O$ phase had been produced above 400°C and then came out from the coating, leading also to reduction of the linkage between metallic particles inside the coating. Therefore, the weight loss could be contributed by explained by both physical abrasion and self-separation (of metallic particles).

As can be seen in Figure 5, sealed NiCr20 coating samples had higher abrasion resistant than that of unsealed samples. At 400°C, the sealed NiCr coating has the highest value of abrasion resistant. Its weight loss (9.8 mg) was 12 times lower than that of unseal coatings (126.3 mg). This finding was also coherent with the XRD analysis and microhardness study. In the sealed coatings, both crystalline phases of $Al_2P_6O_{18}$ and $H_2AlP_3O_{10}$ have significantly contributed to their increase of wear resistance. Moreover, sealed coatings have lower porosity than the unsealed ones (Figure 6) and thus their abrasion resistance might increase.

3.4. Corrosion Test. This section examines the effect of aluminum phosphate on corrosion behavior of prepared coatings. For the comparative study, two samples of NA4 (sealed and treated at 400°C) and NC (unsealed, without heat treatment) have been selected for evaluation.

Figures 7(a) and 7(b) present the EIS data of coatings after 2 hours of immersion in H_2SO_4 solution (pH 2) under the Nyquist and Bode plots, respectively. It was reported in literature that impedance at low frequency can represent the corrosion process of coated steel. As seen in Figure 7(b), at the low frequency, the impedance $|Z|$ of NA4 sample was higher than that of NC sample. This indicated that the corrosion resistance of NA4 coating was higher than that of NC coating. By sealing of aluminum phosphate, the porosity of NA4 coating became lower, thus inhibiting the penetration

Table 8: Values of R_p, i_{corr}, E_{corr} for coatings after 2 hours of immersion in H_2SO_4 solution (pH 2).

Samples	R_p (kΩ.cm^2)	i_{corr} (μA.cm^{-2})	E_{corr} (V/SCE)
NC	7.43	1.07	-0.287
NA4	28.33	0.42	-0.272

of H_2SO_4 solution into the steel substrate. In addition, the arcs in Figure 7(a) could be attributed to several processes, such as (i) oxidation process of coating, (ii) charge transfer process of hydrogen reduction reaction (in acidic solution), and (iii) electrochemical reactions in the pores.

In case of plasma-sprayed alumina coating, Vetrivendan et al. [19] recently also used the aluminum phosphate sealing to improve insulation resistance of their alumina coating. In their study, three values of concentrations of P/Al (molar ratio) were 3, 10, and 15. The authors found that sealing with P/Al molar ratio 3 showed the maximum insulation resistance (~10^{13} Ω). In this work, the polarization resistance (R_p) of coatings could be measured by using the polarization curves. From the data of polarization curves, both corrosion current (i_{corr}) and corrosion potential (E_{corr}) could be calculated.

The polarization curves of coatings after 2 hours of immersion (in H_2SO_4 solution at pH 2) are presented in Figure 8. Table 8 presents the values of R_p, i_{corr} and E_{corr}, which were calculated from polarization curves using AUTOLAB software. As shown in this Table, the corrosion current density (i_{corr}) of NA4 sample (0.42 μA.cm^{-2}) was 2.6 times lower than that of NC sample (1.07 μA.cm^{-2}). Thus, sealed NiCr alloy coating offers more protection against corrosion than the unsealed coating.

4. Conclusions

The main findings of this research were as follows.

(i) After post-heat treatment, XRD studies indicated the formation of various crystalline phases of aluminum phosphate. The presence of $Al_2P_6O_{18}$ crystal component in sealed NiCr coating might contribute to the improvement of its wear resistance. At 1000°C, the aluminum phosphate could be chemically reacted with NiCr alloy coating to form the $Ni_3(PO_4)_2$ (Monoclinic) phase.

(ii) The porosity of aluminum phosphate sealed NiCr alloy coating (with 2.3 molar ratio of P/Al) decreased with increasing the annealing temperature. More than 90% of inherent pores have been sealed after annealing at temperature in range from 800 to 1000°C.

(iii) The abrasion resistance of NiCr coating significantly decreased with increasing the annealing temperature. After heat treatment at 400°C, the abrasion resistance of aluminum phosphate sealed NiCr coating obtained the highest value, which was 12 times higher than that without heat treatment.

(iv) In H_2SO_4 solution at pH 2, the corrosion resistance of aluminum phosphate sealed NiCr alloy coating is much higher as compared to the unsealed coating.

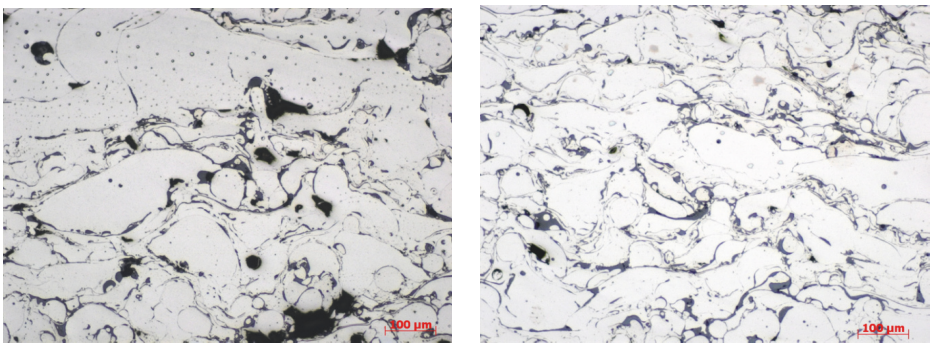

(a) (b)

Figure 6: Cross-sectional structure of NiCr alloy coating unsealed (a) and sealed (b) with aluminum phosphate.

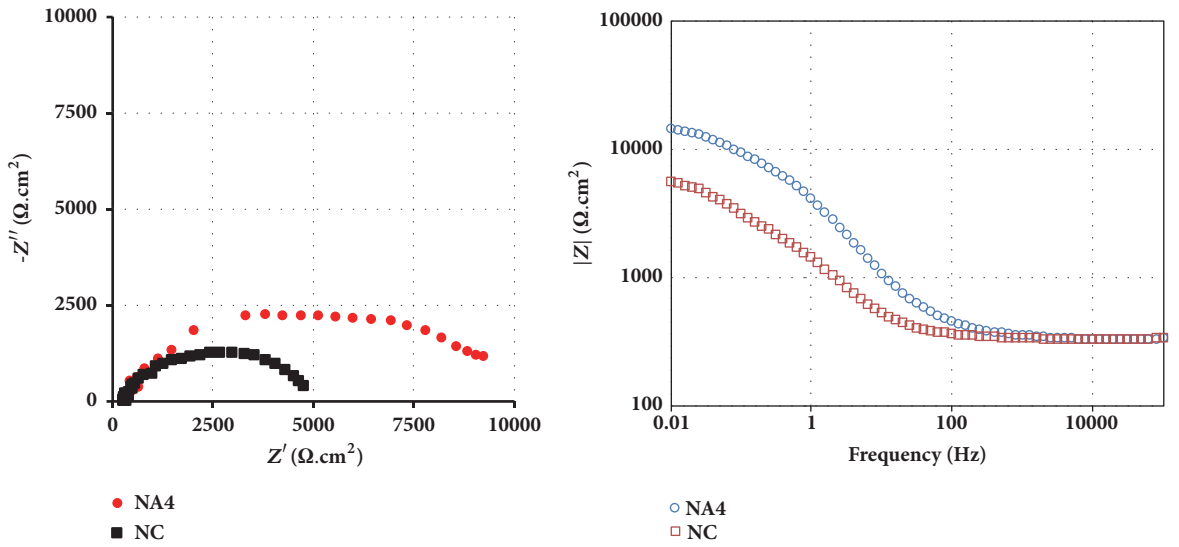

(a) (b)

Figure 7: Nyquist (a) and Bode (b) plots of NC and NA4 coating samples after 2 hours of immersion in H_2SO_4 solution (pH 2).

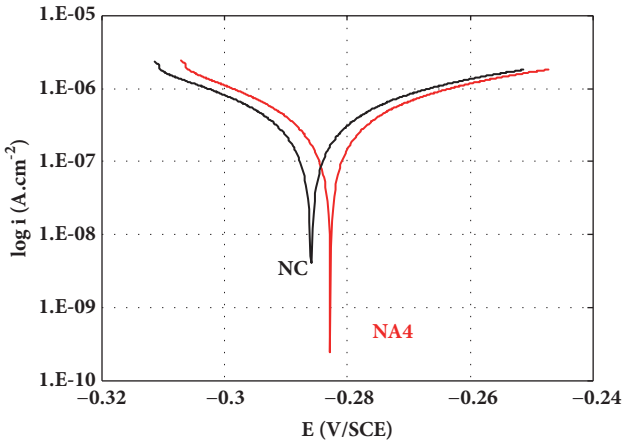

Figure 8: Polarization curves of NC and NA4 coating samples after 2 hours of immersion in H_2SO_4 solution (pH 2).

Data Availability

The data used to support the findings of this study are available from the corresponding author upon request.

Disclosure

A preliminary version of this work had been presented as a poster at the "8th Asian Thermal Spray Conference, Jeju, South Korea, 2017" (Poster P00062).

Conflicts of Interest

The authors declare that there are no conflicts of interest regarding the publication of this paper.

Acknowledgments

This research was funded by Vietnam National Foundation for Science and Technology Development (NAFOSTED) under Grant no. 104.05-2011.38.

References

[1] J. Knuuttila, P. Sorsa, and T. Mäntylä, "Sealing of thermal spray coatings by impregnation," *Journal of Thermal Spray Technology*, vol. 8, no. 2, pp. 249–257, 1999.

[2] K. Niemi, P. Sorsa, P. Vuoristo, and T. Mantyla, "Thermally sprayed alumina coatings with strongly improved wear and corrosion resistance," in *Thermal Spray Industrial Applications*, C. C. Berndt and S. Sampath, Eds., pp. 533–536, ASM International, Materials Park, OH, USA, 1994.

[3] K. Kumpulainen, M. Vippola, K. Niemi, P. Sorsa, P. Vuoristo, and T. Mantyla, "Characteristics of aluminum phosphate sealed chromium oxide coatings," in *Thermal Spray Science and Technology*, C. C. Berndt and S. Sampath, Eds., pp. 579–582, ASM International, Materials Park, OH, USA, 1995.

[4] E. Leivo, M. Vippola, P. Sorsa, P. Vuoristo, and T. Mantyla, "Wear and corrosion properties of plasma sprayed Al_2O_3 and Cr_2O_3 coatings sealed by aluminum phosphates," *Journal of Thermal Spray Technology*, vol. 6, no. 2, pp. 205–210, 1997.

[5] M. Vippola, P. Vuoristo, T. Lepistö, and T. Mäntylä, "AEM study of aluminum phosphate sealed plasma sprayed Al_2O_3 and Cr_2O_3 coatings," *Journal of Materials Science Letters*, vol. 22, no. 6, pp. 463–466, 2003.

[6] G. Berard, P. Brun, J. Lacombe, G. Montavon, A. Denoirjean, and G. Antou, "Influence of a sealing treatment on the behavior of plasma-sprayed alumina coatings operating in extreme environments," *Journal of Thermal Spray Technology*, vol. 17, no. 3, pp. 410–419, 2008.

[7] F. Shao, K. Yang, H. Zhao, Ch. Liu, L. Wang, and S. Tao, "Effects of inorganic sealant and brief heat treatments on corrosion behavior of plasma sprayed Cr_2O_3-Al_2O_3 composite ceramic coatings," *Surface & Coatings Technology*, vol. 276, pp. 8–15, 2015.

[8] A. Frolov, M. Trofimov, and E. Verenkova, "Gas- flame spraying of coatings from ZrO_2 and Al_2O_3 doped with aluminum phosphate," *Chemical Abstracts*, vol. 68, Article ID 52889, 1968.

[9] W. Koenig and G. Cope, "Refractory coating for furnace blowing lances," *Chemical Abstracts*, vol. 68, Article ID 52889v, 1968.

[10] N. Silina and R. Sagitullin, "Refractory coating on metal," *Chemical Abstracts*, vol. 71, Article ID 128162, 1969.

[11] S. Menargues, J. A. Picas, E. Martin, B. P. Maria Teresa, M. Campillo, and A. Forn, "Surface finish effect on the anodizing behaviour of Al-Si components obtained by sub-liquidus casting process," *International Journal of Material Forming*, vol. 2, Supplement 1, pp. 225–228, 2009.

[12] J. Lesage, M. H. Staia, D. Chicot, C. Godoy, and P. E. V. De Miranda, "Effect of thermal treatments on adhesive properties of a NiCr thermal sprayed coating," *Thin Solid Films*, vol. 377-378, pp. 681–686, 2000.

[13] M. Prudenziati and M. L. Gualtieri, "Electrical properties of thermally sprayed Ni- and Ni20Cr-based resistors," *Journal of Thermal Spray Technology*, vol. 17, no. 3, pp. 385–394, 2008.

[14] L. He, D. Chen, and S. Shang, "Fabrication and wear properties of Al_2O_3-SiC ceramic coatings using aluminum phosphate as binder," *Journal of Materials Science*, vol. 39, no. 15, pp. 4887–4892, 2004.

[15] B. M. Amokrane, A. Abdelhamid, M. Youcef, B. Abderrahim, O. Nedjeddine, and M. Ahmed, "Microstructural and mechanical properties of Ni-base thermal spray coatings deposited by flame spraying," *Metallurgical and Materials Transactions B: Process Metallurgy and Materials Processing Science*, vol. 42, no. 5, pp. 932–938, 2011.

[16] Y. Wang, S. L. Jiang, Y. G. Zheng, W. Ke, W. H. Sun, and J. Q. Wang, "Effect of porosity sealing treatments on the corrosion resistance of high-velocity oxy-fuel (HVOF)-sprayed Fe-based amorphous metallic coatings," *Surface and Coatings Technology*, vol. 206, no. 6, pp. 1307–1318, 2011.

[17] M. E. Aalamialeagha, S. J. Harris, and M. Emamighomi, "Influence of the HVOF spraying process on the microstructure and corrosion behaviour of Ni-20%Cr coatings," *Journal of Materials Science*, vol. 38, no. 22, pp. 4587–4596, 2003.

[18] A. Durif, *Crystal Chemistry of Condensed Phosphates*, Plenum Press, New York, NY, USA, 1995.

[19] E. Vetrivendan, G. Thendral, A. R. Shankar, C. Mallika, and U. Kamachi Mudali, "Aluminum phosphate sealing to improve insulation resistance of plasma-sprayed alumina coating," *Materials and Manufacturing Processes*, vol. 32, no. 12, pp. 1435–1441, 2017.